PERGAMON

International Journal of Solids and Structures 38 (2001) 2933–2952

INTERNATIONAL JOURNAL OF SOLIDS and STRUCTURES

www.elsevier.com/locate/ijsolstr

A thermodynamically consistent approach to microplane theory. Part II. Dissipation and inelastic constitutive modeling

Ellen Kuhl [a], Paul Steinmann [b], Ignacio Carol [c,*]

[a] *Institute of Structural Mechanics, University of Stuttgart, Pfaffenwaldring 7, D-70550 Stuttgart, Germany*
[b] *Chair for Applied Mechanics, University of Kaiserslautern, Postfach 3049, D-67653 Kaiserslautern, Germany*
[c] *School of Civil Engineering (ETSECCPB), Technical University of Catalonia (UPC), E-08034 Barcelona, Spain*

Received 12 June 1999; in revised form 16 April 2000

Abstract

The main objective of the present work is to provide a general framework for constitutive laws based on the microplane theory applicable to any kind of rheological behavior. Therefore, a thermodynamically consistent concept of deriving microplane based constitutive equations is presented. Microscopic constitutive laws are formulated on characteristic material planes, the so-called microplanes, resulting in an overall anisotropic macroscopic material characterization. The microscopic strain components of one plane are derived by the projection of the macroscopic strain tensor, leading to a kinematically constrained model. As proposed in the first part of this paper, the introduction of individual potentials on each microplane yields thermodynamically consistent microplane laws. They can be related to the macroscopic material description through an integration over the hemisphere. The microplane laws are chosen such that the macroscopic version of the Clausius–Duhem inequality is satisfied. This generic concept will be applied to the classical models of elasticity, elasto-damage and elasto-plasticity. The results are documented by the analysis of pointwise texture evolution for the model problems of uniaxial tension and simple shear.

Keywords: Microplane theory; Elasto-damage; Elasto-plasticity; Anisotropy

1. Introduction

For a wide class of materials, the assumption of isotropic material response yields sufficiently accurate results. Nevertheless, for heterogeneous materials, e.g. concrete or other composites, the assumption of isotropy is no longer valid, since microcracks and microvoids will develop anisotropically under increased loading. Moreover, metallic materials may show an anisotropic response due to their crystalline microstructure.

The modeling of inelastic isotropic material behavior is nowadays well-understood, especially because only a few material parameters are needed to simulate either damage or plasticity (e.g. Lemaitre and

* Corresponding author. Fax: +34-93-401-7251.
E-mail address: ignacio.carol@upc.es (I. Carol).

0020-7683/01/$ - see front matter
PII: S0020-7683(00)00213-4

Chaboche, 1985). The constitutive modeling of anisotropy, however, is far more difficult and the understanding and identification of material parameters is a sophisticated task (Carol et al., 2000b). A general concept to model anisotropic material behavior has been proposed by Taylor (1938), who suggested to consider the uniaxial material response on several characteristic material planes. A clear advantage of this concept is that the material properties can be directly related to the behavior under uniaxial loading. At first, Taylor's ideas were only related to crystal plasticity, where plastic sliding was assumed to take place on several slip planes, defined by the geometry of the crystalline lattice (Batdorf and Budiansky, 1949). It was only during the last decade that the general idea of Taylor was applied to continuum damage mechanics by Bažant and Gambarova (1984), Bažant and Prat (1988), Carol et al. (1991, 1992). The generic name "microplane theory" was coined in order to demonstrate that the concept of defining constitutive laws on characteristic material planes was not restricted to plasticity but could be applied to any kind of material behavior.

Nevertheless, the thermodynamically consistent formulation of a general strategy of deriving microplane based constitutive models is still an open issue. Most existing microplane models are mainly based on the so-called kinematic constraint, such that the microplane strains are determined by a projection of the overall strain tensor. In former formulations, however, the microplane stresses were related to the overall stress tensor by the equivalence of virtual work (Bažant and Prat, 1988). These relations, were rather motivated by phenomenological considerations, but nevertheless, they yielded excellent results when modeling the brittle failure of concrete (Ožbolt and Bažant, 1992; Bažant and Planas, 1998). A natural consequence of these phenomenological models is that they may result in non-symmetric material operators. Furthermore, the satisfaction of the second principle of thermodynamics cannot automatically be guaranteed for this class of models, as demonstrated in part I of this paper (Carol et al., 2000a). There, it was proposed that thermodynamically consistent microplane-based constitutive equations can be derived by introducing a microscopic free Helmholtz energy on every microplane. In this second part, we will focus on inelastic material behavior. When assuming an appropriate relation between these microscopic free energies and the macroscopic free energy, we can evaluate the Clausius–Duhem inequality according to Coleman's method in the same fashion as for classical thermodynamically consistent constitutive laws. This general approach can be applied not only to microplane elasticity but to all kinds of material behavior, including elasticity, damage and plasticity and combinations thereof.

The paper is organized as follows: In Section 2, we briefly summarize the purely geometric relations based on a kinematic and static constraint. After demonstrating a general concept of deriving constitutive formulations motivated by the microplane idea in Section 3, we will include a brief discussion on the relation of the macroscopic stress power to several different microscopic stress power definitions in Section 4. Finally, we will recapitulate the application of the microplane concept to elastic material models in Section 5. The extension to inelastic material behavior will be demonstrated by the application to elasto-damage models in Section 6 and finally to elasto-plastic models in Section 7. The different material formulations will be examined by means of the model problems of pointwise uniaxial tension and simple shear. Due to the underlying microplane structure, it is possible to visualize the development of anisotropy and texture evolution in terms of the microplane components.

2. Kinematic and static constraint for one microplane

2.1. Macroscopic strain and stress tensor

To set the stage, we briefly reiterate the boundary value problem of geometrically linear continuum mechanics. Let $\mathscr{B} \subset \mathbb{R}^{n_{\text{dim}}}$ denote the configuration occupied by the solid with placements in $\mathbb{R}^{n_{\text{dim}}}$ denoted by x. The boundary $\partial\mathscr{B}$ of $\mathscr{B}$ is subdivided into disjoint parts $\partial\mathscr{B} = \partial\mathscr{B}_u \cup \partial\mathscr{B}_t$ with $\partial\mathscr{B}_u \cap \partial\mathscr{B}_t = \emptyset$, where

either Dirichlet or Neumann boundary conditions are prescribed. Deformations of the solid are described by the displacement field $u : \mathscr{B} \rightarrow \mathbb{R}^{n_{\text{dim}}}$, distributed body forces per unit volume are given by the vector field $\boldsymbol{f} : \mathscr{B} \rightarrow \mathbb{R}^{n_{\text{dim}}}$. The symmetric tensor fields of the macroscopic stresses and strains are introduced as $\boldsymbol{\sigma} : \mathscr{B} \rightarrow \mathbb{R}^{n_{\text{dim}} \times n_{\text{dim}}}$ and $\boldsymbol{\epsilon} : \mathscr{B} \rightarrow \mathbb{R}^{n_{\text{dim}} \times n_{\text{dim}}}$. With the assumption of small strains, the macroscopic strain tensor $\boldsymbol{\epsilon}$ can be expressed as the symmetric part of the displacement gradient ∇u.

$$\boldsymbol{\epsilon} = \nabla^{\text{sym}} \boldsymbol{u}. \tag{1}$$

At equilibrium, the macroscopic stress tensor $\boldsymbol{\sigma}$ satisfies the balance of linear momentum

$$\text{div}\,\boldsymbol{\sigma} = -\boldsymbol{f} \tag{2}$$

in the domain $\mathscr{B}$ and is specified by the constitutive equation $\boldsymbol{\sigma} = \hat{\boldsymbol{\sigma}}(\boldsymbol{\epsilon}, \boldsymbol{q})$ with $\boldsymbol{q}$ denoting a vector of internal variables.

2.2. Microscopic strain and stress components

The macroscopic strain and stress tensor may be related to microscopic strain and stress components by a kinematic or a static constraint, requiring that either the strains or the stresses of each microplane can be derived by projections of their macroscopic counterparts, respectively.

$$\begin{aligned} \epsilon_{\text{V}} &= \boldsymbol{V} : \boldsymbol{\epsilon}, & \bar{\sigma}_{\text{V}} &= \boldsymbol{V} : \boldsymbol{\sigma}, \\ \epsilon_{\text{D}} &= \boldsymbol{D} : \boldsymbol{\epsilon}, & \bar{\sigma}_{\text{D}} &= \boldsymbol{D} : \boldsymbol{\sigma}, \\ \boldsymbol{\epsilon}_{\text{T}} &= \boldsymbol{T} : \boldsymbol{\epsilon}, & \bar{\boldsymbol{\sigma}}_{\text{T}} &= \boldsymbol{T} : \boldsymbol{\sigma}. \end{aligned} \tag{3}$$

Herein, ϵ_{V} and ϵ_{D} are the volumetric and the deviatoric components of the normal strain and $\boldsymbol{\epsilon}_{\text{T}}$ denotes the tangential strain vector, respectively. Correspondingly, the volumetric and the deviatoric projected microscopic stresses and the projected tangential stress vector are represented by $\bar{\sigma}_{\text{V}}$, $\bar{\sigma}_{\text{D}}$ and $\bar{\boldsymbol{\sigma}}_{\text{T}}$. Note that these projected stress components might in general be different from the constitutive stress components derived from the constitutive equations, which will be denoted by σ_{V}, σ_{D} and $\boldsymbol{\sigma}_{\text{T}}$ in the following. According to Fig. 1, the strain vector $\boldsymbol{t}_{\epsilon}$ and the projected stress vector $\bar{\boldsymbol{t}}_{\sigma}$ associated with the corresponding plane can be expressed as projections of the strain tensor $\boldsymbol{\epsilon}$ and the stress tensor $\boldsymbol{\sigma}$ by the plane's normal $\boldsymbol{n}$. They are related to the individual microplane components introduced in Eq. (3) in the following form:

$$\begin{aligned} \boldsymbol{t}_{\epsilon} &= \boldsymbol{\epsilon} \cdot \boldsymbol{n} = [\epsilon_{\text{V}} + \epsilon_{\text{D}}]\boldsymbol{n} + \boldsymbol{\epsilon}_{\text{T}}, \\ \bar{\boldsymbol{t}}_{\sigma} &= \boldsymbol{\sigma} \cdot \boldsymbol{n} = [\bar{\sigma}_{\text{V}} + \bar{\sigma}_{\text{D}}]\boldsymbol{n} + \bar{\boldsymbol{\sigma}}_{\text{T}}. \end{aligned} \tag{4}$$

The individual projection tensors $\boldsymbol{V}$, $\boldsymbol{D}$ and $\boldsymbol{T}$ of Eq. (3) are characterized by the plane's normal $\boldsymbol{n}$ as well as the second-order identity tensor $\mathbf{1}$ with coefficients δ_{IJ} and the symmetric part of the fourth-order identity tensor $\mathscr{I}$ with coefficients $[\delta_{IK}\delta_{JL} + \delta_{IL}\delta_{JK}]/2$. Herein, $\mathscr{I}$ can be additively decomposed into a volumetric and a deviatoric part, $\mathscr{I} = \mathscr{I}_{\text{vol}} + \mathscr{I}_{\text{dev}}$ with $\mathscr{I}_{\text{vol}} = 1/3\ \mathbf{1} \otimes \mathbf{1}$ and $\mathscr{I}_{\text{dev}} = \mathscr{I} - 1/3\ \mathbf{1} \otimes \mathbf{1}$.

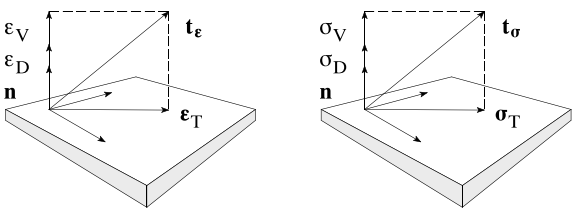

Fig. 1. Strain and stress components on one microplane.

$$\begin{aligned} \boldsymbol{V} &= \tfrac{1}{3}\,\mathbf{1}, \\ \boldsymbol{D} &= \boldsymbol{n}\otimes\boldsymbol{n} - \tfrac{1}{3}\,\mathbf{1}, \\ \boldsymbol{T} &= \boldsymbol{n}\cdot\boldsymbol{\mathcal{I}} - \boldsymbol{n}\otimes\boldsymbol{n}\otimes\boldsymbol{n}. \end{aligned} \tag{5}$$

Note that the premultiplication with the third-order tensor $\boldsymbol{T}$ maps a second-order tensor to a vector in the plane, whereas a postmultiplication with $\boldsymbol{T}$ of a vector in the plane yields a symmetric, second-order tensor. The latter mapping of the vector in the plane $\boldsymbol{v}$, which is orthogonal to the plane's normal $\boldsymbol{n}$ such that $\boldsymbol{v}\cdot\boldsymbol{n}=0$ can be rewritten in the following simple form:

$$\boldsymbol{v}\cdot\boldsymbol{T} = [\boldsymbol{v}\otimes\boldsymbol{n}]^{\mathrm{sym}} + [\boldsymbol{v}\cdot\boldsymbol{n}]\boldsymbol{n}\otimes\boldsymbol{n} = [\boldsymbol{v}\otimes\boldsymbol{n}]^{\mathrm{sym}}. \tag{6}$$

According to Bažant and Oh (1985) and Lubarda and Krajcinovic (1993), the following integration properties of the normal vector $\boldsymbol{n}$ can be applied to perform an analytical integration over the entire hemisphere Ω:

$$\begin{aligned} &\int_{\Omega} \mathrm{d}\Omega = 2\pi, \\ &\int_{\Omega} \boldsymbol{n}\otimes\boldsymbol{n}\,\mathrm{d}\Omega = \tfrac{2\pi}{3}\,\mathbf{1}, \\ &\int_{\Omega} \boldsymbol{n}\otimes\boldsymbol{n}\otimes\boldsymbol{n}\otimes\boldsymbol{n}\,\mathrm{d}\Omega = \tfrac{2\pi}{3}\left[\boldsymbol{\mathcal{I}}_{\mathrm{vol}} + \tfrac{2}{5}\boldsymbol{\mathcal{I}}_{\mathrm{dev}}\right]. \end{aligned} \tag{7}$$

With the help of the above equations, the dyadic products of the projection tensors $\boldsymbol{V}$, $\boldsymbol{D}$ and $\boldsymbol{T}$ show the following properties when integrated analytically over the hemisphere:

$$\begin{aligned} &\tfrac{3}{2\pi}\int_{\Omega} \boldsymbol{V}\otimes\boldsymbol{V}\,\mathrm{d}\Omega = \boldsymbol{\mathcal{I}}_{\mathrm{vol}}, \\ &\tfrac{3}{2\pi}\int_{\Omega} \boldsymbol{D}\otimes\boldsymbol{D}\,\mathrm{d}\Omega = \tfrac{2}{5}\boldsymbol{\mathcal{I}}_{\mathrm{dev}}, \\ &\tfrac{3}{2\pi}\int_{\Omega} \boldsymbol{T}^{\mathrm{T}}\cdot\boldsymbol{T}\,\mathrm{d}\Omega = \tfrac{3}{5}\boldsymbol{\mathcal{I}}_{\mathrm{dev}}. \end{aligned} \tag{8}$$

Note that an integral orthogonality holds for the volumetric and the deviatoric projection tensors,

$$\begin{aligned} &\tfrac{3}{2\pi}\int \Omega\boldsymbol{V}\otimes\boldsymbol{D}\,\mathrm{d}\Omega = \mathbf{0}, \\ &\tfrac{3}{2\pi}\int \Omega\boldsymbol{D}\otimes\boldsymbol{V}\,\mathrm{d}\Omega = \mathbf{0}. \end{aligned} \tag{9}$$

3. Thermodynamically consistent constitutive laws

A possible drawback of the original microplane models is that they are not derived from a potential and consequently, do not necessarily result in symmetric material operators (Bažant and Prat, 1988). The present contribution aims at providing a general formalism of deriving thermodynamically consistent microplane-based constitutive laws. The macroscopic Clausius–Duhem inequality for the isothermal case

$$\mathscr{D}^{\mathrm{mac}} = \boldsymbol{\sigma} : \dot{\boldsymbol{\epsilon}} - \dot{\Psi}^{\mathrm{mac}} \geqslant 0 \tag{10}$$

serves as starting point for the derivation of our constitutive formulation. If we apply the following assumption according to Carol et al. (2000a),

$$\Psi^{\mathrm{mac}} = \frac{3}{2\pi} \int_{\Omega} \Psi^{\mathrm{mic}} \mathrm{d}\Omega, \tag{11}$$

the macroscopic and the microscopic free energy Ψ^{mac} and Ψ^{mic} can be related in an integral sense. Furthermore, a constitutive assumption for the microscopic free energy Ψ^{mic} of one plane has to be made. In its general form, the microscopic free energy depends on the strain components ϵ_{V}, ϵ_{D} and $\boldsymbol{\epsilon}_{\mathrm{T}}$ as well as on a set of internal variables collected in the vector $\boldsymbol{q}$,

$$\Psi^{\mathrm{mic}} = \hat{\Psi}^{\mathrm{mic}}(\epsilon_{\mathrm{V}}, \epsilon_{\mathrm{D}}, \boldsymbol{\epsilon}_{\mathrm{T}}, \boldsymbol{q}). \tag{12}$$

With the help of the kinematic constraint of Eq. (3), the evolution of the microscopic free energy can be written as follows:

$$\dot{\Psi}^{\mathrm{mic}} = \left[\boldsymbol{V}\sigma_{\mathrm{V}} + \boldsymbol{D}\sigma_{\mathrm{D}} + \boldsymbol{T}^{\mathrm{T}} \cdot \boldsymbol{\sigma}_{\mathrm{T}} \right] : \dot{\boldsymbol{\epsilon}} - \mathscr{D}^{\mathrm{mic}}, \tag{13}$$

whereby σ_{V}, σ_{D} and $\boldsymbol{\sigma}_{\mathrm{T}}$ denote the microscopic constitutive stresses

$$\sigma_{\mathrm{V}} := \frac{\partial \Psi^{\mathrm{mic}}}{\partial \epsilon_{\mathrm{V}}} \qquad \sigma_{\mathrm{D}} := \frac{\partial \Psi^{\mathrm{mic}}}{\partial \epsilon_{\mathrm{D}}} \qquad \boldsymbol{\sigma}_{\mathrm{T}} := \frac{\partial \Psi^{\mathrm{mic}}}{\partial \boldsymbol{\epsilon}_{\mathrm{T}}}, \tag{14}$$

which are, in general, not identical to the projected microscopic stresses defined through the static constraint in Eq. (3). Moreover, $\mathscr{D}^{\mathrm{mic}}$ defines the microscopic dissipation as

$$\mathscr{D}^{\mathrm{mic}} := -\frac{\partial \Psi^{\mathrm{mic}}}{\partial \boldsymbol{q}} \cdot \dot{\boldsymbol{q}}, \tag{15}$$

with $\cdot$ denoting the scalar product of the order of $\boldsymbol{q}$. When including the evolution of the microscopic free energy of Eq. (13) in the integral relation (11), we obtain the evolution equation for the macroscopic free energy as

$$\dot{\Psi}^{\mathrm{mac}} = \frac{3}{2\pi} \int_{\Omega} \left[\boldsymbol{V}\sigma_{\mathrm{V}} + \boldsymbol{D}\sigma_{\mathrm{D}} + \boldsymbol{T}^{\mathrm{T}} \cdot \boldsymbol{\sigma}_{\mathrm{T}} \right] \mathrm{d}\Omega : \dot{\boldsymbol{\epsilon}} - \frac{3}{2\pi} \int_{\Omega} \mathscr{D}^{\mathrm{mic}} \mathrm{d}\Omega. \tag{16}$$

Finally, the macroscopic version of the Clausius–Duhem inequality (10) can be evaluated, yielding the definition of the macroscopic stress tensor $\boldsymbol{\sigma}$ in terms of the microscopic constitutive stress components, compare Eq. (14) of Part I (Carol et al., 2000a),

$$\boldsymbol{\sigma} = \frac{3}{2\pi} \int_{\Omega} \left[\boldsymbol{V}\sigma_{\mathrm{V}} + \boldsymbol{D}\sigma_{\mathrm{D}} + \boldsymbol{T}^{\mathrm{T}} \cdot \boldsymbol{\sigma}_{\mathrm{T}} \right] \mathrm{d}\Omega. \tag{17}$$

Next, in order to fulfill the macroscopic dissipation inequality

$$\mathscr{D}^{\mathrm{mac}} = \frac{3}{2\pi} \int_{\Omega} \mathscr{D}^{\mathrm{mic}} \mathrm{d}\Omega \geqslant 0, \tag{18}$$

we will require that the microscopic energy dissipation on every plane is non-negative.

$$\mathscr{D}^{\mathrm{mic}} \geqslant 0. \tag{19}$$

This requirement is obviously stronger than the requirement posed by Eq. (18) and therefore, represents a sufficient condition to fulfill the second principle of thermodynamics. Thus, Eq. (13) can be interpreted as a microscopic version of the Clausius–Duhem inequality, such that

$$\mathscr{D}^{\mathrm{mic}} = \mathscr{P}^{\mathrm{mic}} - \dot{\Psi}^{\mathrm{mic}} \geqslant 0 \quad \text{with } \mathscr{P}^{\mathrm{mic}} := \sigma_{\mathrm{V}}\dot{\epsilon}_{\mathrm{V}} + \sigma_{\mathrm{D}}\dot{\epsilon}_{\mathrm{D}} + \boldsymbol{\sigma}_{\mathrm{T}} \cdot \dot{\boldsymbol{\epsilon}}_{\mathrm{T}}. \tag{20}$$

The following examples will demonstrate that the tangent operator $\boldsymbol{E}_{\mathrm{t}}$ relating the stress rate and the strain rate with $\dot{\boldsymbol{\sigma}} = \boldsymbol{E}_{\mathrm{t}} : \dot{\boldsymbol{\epsilon}}$

$$\boldsymbol{\sigma} = \frac{\partial \Psi^{\mathrm{mac}}}{\partial \boldsymbol{\epsilon}} \quad \rightarrow \boldsymbol{E}_{\mathrm{t}} = \frac{\mathrm{d}\boldsymbol{\sigma}}{\mathrm{d}\boldsymbol{\epsilon}} = \frac{3}{2\pi} \int_{\Omega} \left[\boldsymbol{V} \otimes \frac{\mathrm{d}\sigma_{\mathrm{V}}}{\mathrm{d}\boldsymbol{\epsilon}} + \boldsymbol{D} \otimes \frac{\mathrm{d}\sigma_{\mathrm{D}}}{\mathrm{d}\boldsymbol{\epsilon}} + \boldsymbol{T}^{\mathrm{T}} \cdot \frac{\mathrm{d}\boldsymbol{\sigma}_{\mathrm{T}}}{\mathrm{d}\boldsymbol{\epsilon}} \right] \mathrm{d}\Omega, \tag{21}$$

becomes symmetric due to the derivation based on a stress potential. The numerical evaluation of the constitutive law is described in detail in Appendix A.

4. Remarks on macroscopic and microscopic stress power

The scalar product of the macroscopic stress tensor $\boldsymbol{\sigma}$ and the strain rate tensor $\dot{\boldsymbol{\epsilon}}$ yields the macroscopic stress power $\mathscr{P}^{\mathrm{mac}}$,

$$\mathscr{P}^{\mathrm{mac}} = \boldsymbol{\sigma} : \dot{\boldsymbol{\epsilon}}. \tag{22}$$

In analogy to this macroscopic stress power, a microscopic stress power $\bar{\mathscr{P}}^{\mathrm{mic}}$ based on the projected stresses can be identified as the scalar product of the projected stress vector $\bar{\boldsymbol{t}}_{\sigma}$ and the strain rate vector $\dot{\boldsymbol{t}}_{\epsilon}$. With the help of the kinematic and static constraint (4), this microscopic stress power can thus be expressed as follows:

$$\bar{\mathscr{P}}^{\mathrm{mic}} = \bar{\boldsymbol{t}}_{\sigma} \cdot \dot{\boldsymbol{t}}_{\epsilon} = [\boldsymbol{\sigma} \cdot \dot{\boldsymbol{\epsilon}}] : [\boldsymbol{n} \otimes \boldsymbol{n}]. \tag{23}$$

Its integration over the hemisphere Ω

$$\frac{3}{2\pi} \int_{\Omega} \bar{\mathscr{P}}^{\mathrm{mic}} \, \mathrm{d}\Omega = \frac{3}{2\pi} \int_{\Omega} [\boldsymbol{\sigma} \cdot \dot{\boldsymbol{\epsilon}}] : [\boldsymbol{n} \otimes \boldsymbol{n}] \, \mathrm{d}\Omega = \boldsymbol{\sigma} : \dot{\boldsymbol{\epsilon}} \tag{24}$$

as depicted in Fig. 2 yields the integral relation between the macroscopic and the microscopic stress power,

$$\mathscr{P}^{\mathrm{mac}} = \frac{3}{2\pi} \int_{\Omega} \bar{\mathscr{P}}^{\mathrm{mic}} \mathrm{d}\Omega \quad \text{with } \bar{\mathscr{P}}^{\mathrm{mic}} = \bar{\sigma}_{\mathrm{V}} \dot{\epsilon}_{\mathrm{V}} + \bar{\sigma}_{\mathrm{D}} \dot{\epsilon}_{\mathrm{V}} + \bar{\sigma}_{\mathrm{V}} \dot{\epsilon}_{\mathrm{D}} + \bar{\sigma}_{\mathrm{D}} \dot{\epsilon}_{\mathrm{D}} + \bar{\boldsymbol{\sigma}}_{\mathrm{T}} \cdot \dot{\boldsymbol{\epsilon}}_{\mathrm{T}}. \tag{25}$$

Herein, we have made use of the kinematic relations (4) which define the strain vector and the projected stress vector in terms of their microscopic components. With the help of the analytical integration formulae

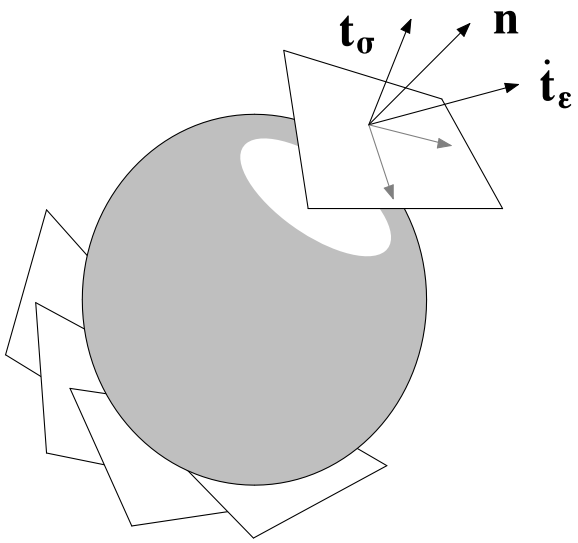

Fig. 2. Evaluation of microscopic stress power on individual planes.

derived in Eq. (9), we observe that the mixed terms of the above equation yield no contribution to the macroscopic stress power. Thus,

$$\begin{aligned} \tfrac{3}{2\pi}\int_\Omega \bar{\sigma}_V \dot{\epsilon}_D \, d\Omega = \boldsymbol{\sigma} : \tfrac{3}{2\pi}\int_\Omega [\boldsymbol{V} \otimes \boldsymbol{D}] \, d\Omega : \dot{\boldsymbol{\epsilon}} = 0, \\ \tfrac{3}{2\pi}\int_\Omega \bar{\sigma}_D \dot{\epsilon}_V \, d\Omega = \boldsymbol{\sigma} : \tfrac{3}{2\pi}\int_\Omega [\boldsymbol{D} \otimes \boldsymbol{V}] \, d\Omega : \dot{\boldsymbol{\epsilon}} = 0. \end{aligned} \tag{26}$$

We can thus simplify Eq. (25) as

$$\mathscr{P}^{mac} = \frac{3}{2\pi}\int_\Omega \tilde{\mathscr{P}}^{mic} d\Omega \quad \text{with} \quad \tilde{\mathscr{P}}^{mic} := \bar{\sigma}_V \dot{\epsilon}_V + \bar{\sigma}_D \dot{\epsilon}_D + \bar{\boldsymbol{\sigma}}_T \cdot \dot{\boldsymbol{\epsilon}}_T. \tag{27}$$

$\tilde{\mathscr{P}}^{mic}$ denotes a redefinition of the microscopic stress power based on the projected microscopic stresses. Moreover, the microscopic stress power $\mathscr{P}^{mic}$ based on the microscopic constitutive stresses as defined in Eq. (20), can be related to the macroscopic stress power through the macroscopic Clausius–Duhem inequality (10), yielding an analogous form,

$$\mathscr{P}^{mac} = \frac{3}{2\pi}\int_\Omega \mathscr{P}^{mic} d\Omega \quad \text{with } \mathscr{P}^{mic} := \sigma_V \dot{\epsilon}_V + \sigma_D \dot{\epsilon}_D + \boldsymbol{\sigma}_T \cdot \dot{\boldsymbol{\epsilon}}_T. \tag{28}$$

In summary, a comparison of the three different stress powers yields the following micro–macro relations:

$$\mathscr{P}^{mac} = \frac{3}{2\pi}\int_\Omega \bar{\mathscr{P}}^{mic} d\Omega = \frac{3}{2\pi}\int_\Omega \tilde{\mathscr{P}}^{mic} d\Omega = \frac{3}{2\pi}\int_\Omega \mathscr{P}^{mic} d\Omega. \tag{29}$$

However, it is important to notice that this relation does not imply that the three different microscopic stress powers are identical on each plane. In general, we observe that

$$\bar{\mathscr{P}}^{mic} \neq \tilde{\mathscr{P}}^{mic}, \quad \tilde{\mathscr{P}}^{mic} \neq \mathscr{P}^{mic}, \quad \mathscr{P}^{mic} \neq \bar{\mathscr{P}}^{mic}, \tag{30}$$

which implies that the projected microscopic stresses are not necessarily identical to the constitutive microscopic stresses,

$$\bar{\sigma}_D \neq \sigma_D, \qquad \bar{\boldsymbol{\sigma}}_T \neq \boldsymbol{\sigma}_T. \tag{31}$$

It should be noted, that the problem associated with decomposition of the macroscopic stress tensor into more than three stress vectors has a non-unique solution. Consequently, there exist infinitely many microplane stress states satisfying the equilibrium equation (2). Thus, the combination of constitutive microplane stresses defined through Eq. (14) represents only one particular solution among infinitely many others. Nevertheless, this choice is in accordance with the macroscopic Clausius–Duhem inequality (10).

5. Microplane elasticity

First, we would like to apply the concepts of Section 3 to microplane elasticity. To describe elastic microplane behavior, no internal variables are necessary, i.e.

$$\boldsymbol{q} \equiv \emptyset. \tag{32}$$

Consequently, the microscopic free energy can be phrased exclusively in terms of the microplane strain components

$$\Psi^{mic} = \hat{\Psi}^{mic}(\epsilon_V, \epsilon_D, \boldsymbol{\epsilon}_T). \tag{33}$$

By introducing E_V and E_D as the volumetric and the deviatoric microscopic elastic moduli and $\boldsymbol{E}_T$ as the second order tensor of the tangential microscopic elastic moduli, we might express the free microscopic energy in the following form:

$$\Psi^{mic} = W_V(\epsilon_V) + W_D(\epsilon_D) + W_T(\boldsymbol{\epsilon}_T) \tag{34}$$

with the microscopic contributions to the stored energy functions W_V, W_D and W_T given as follows:

$$W_V = \tfrac{1}{2}\,\epsilon_V E_V \epsilon_V, \qquad W_D = \tfrac{1}{2}\,\epsilon_D E_D \epsilon_D, \qquad W_T = \tfrac{1}{2}\,\boldsymbol{\epsilon}_T \cdot \boldsymbol{E}_T \cdot \boldsymbol{\epsilon}_T. \tag{35}$$

The evaluation of the microscopic Clausius–Duhem inequality as defined in Eq. (20) yields the definition of the microscopic constitutive stresses as thermodynamically conjugate variables to the individual strain components, i.e.

$$\sigma_V := \frac{\partial \Psi^{mic}}{\partial \epsilon_V} = E_V \epsilon_V, \qquad \sigma_D := \frac{\partial \Psi^{mic}}{\partial \epsilon_D} = E_D \epsilon_D, \qquad \boldsymbol{\sigma}_T := \frac{\partial \Psi^{mic}}{\partial \boldsymbol{\epsilon}_T} = \boldsymbol{E}_T \cdot \boldsymbol{\epsilon}_T. \tag{36}$$

Moreover, the macroscopic Clausius–Duhem inequality renders the definition of the macroscopic stress tensor in terms of the microscopic stress components, i.e.

$$\boldsymbol{\sigma} = \frac{3}{2\pi} \int_\Omega \left[\boldsymbol{V} E_V \epsilon_V + \boldsymbol{D} E_D \epsilon_D + \boldsymbol{T}^T \cdot \boldsymbol{E}_T \cdot \boldsymbol{\epsilon}_T \right] d\Omega. \tag{37}$$

Eq. (37) can thus be rewritten as

$$\boldsymbol{\sigma} = \boldsymbol{E}^{el} : \boldsymbol{\epsilon} \tag{38}$$

with the macroscopic constitutive moduli defined as follows:

$$\boldsymbol{E}^{el} = \frac{3}{2\pi} \int_\Omega \left[E_V \boldsymbol{V} \otimes \boldsymbol{V} + E_D \boldsymbol{D} \otimes \boldsymbol{D} + \boldsymbol{T}^T \cdot \boldsymbol{E}_T \cdot \boldsymbol{T} \right] d\Omega. \tag{39}$$

Remarkably, the tensor of the constitutive moduli is a symmetric tensor, since it has been derived within the framework of thermodynamics. With the additional assumption of microplane isotropy, the tangential strain vector and the tangential stress vector remain parallel during the entire load history. Consequently, we can make use of the following simplification:

$$\boldsymbol{\epsilon}_T \| \boldsymbol{\sigma}_T \rightarrow \boldsymbol{E}_T = E_T\, \boldsymbol{1}. \tag{40}$$

Finally, by assuming that the constitutive moduli are independent from the orientation such that

$$\boldsymbol{E}^{el} = E_V \frac{3}{2\pi} \int_\Omega \boldsymbol{V} \otimes \boldsymbol{V} + E_D \frac{3}{2\pi} \int_\Omega \boldsymbol{D} \otimes \boldsymbol{D} + E_T\, \frac{3}{2\pi} \int_\Omega \boldsymbol{T}^T \cdot \boldsymbol{T} d\Omega, \tag{41}$$

the integrals of Eq. (41) can be evaluated analytically with the help of the integration formulae (8), yielding the following simplified relation:

$$\boldsymbol{E}^{el} = E_V \boldsymbol{\mathcal{I}}_{vol} + \tfrac{2}{5} E_D \boldsymbol{\mathcal{I}}_{dev} + \tfrac{3}{5} E_T \boldsymbol{\mathcal{I}}_{dev}. \tag{42}$$

Herein, $\boldsymbol{E}^{el}$ denotes the fourth-order constitutive tensor. A comparison of the above equations with Hooke's law of elasticity with

$$\boldsymbol{E}^{el} = 3K \boldsymbol{\mathcal{I}}_{vol} + 2G \boldsymbol{\mathcal{I}}_{dev} \tag{43}$$

can be used in order to identify the microscopic constitutive moduli in terms of the macroscopic bulk modulus K and the macroscopic shear modulus G. Thus,

$$E_V = 3K, \qquad \tfrac{2}{5} E_D + \tfrac{3}{5} E_T = 2G. \tag{44}$$

These relations between the microscopic and macroscopic elastic moduli coincide with previous results as given e.g. by Bažant and coworkers (1988, 1998). Note that for microplane elasticity with the special choice of $E_D \equiv E_T = 2G$, we can obtain the only formulation for which the constitutive microscopic stresses are identical to the projected stresses; thus,

$$E_D \equiv E_T = 2G, \quad \sigma_V \equiv \bar{\sigma}_V, \quad \sigma_D \equiv \bar{\sigma}_D, \quad \boldsymbol{\sigma}_T \equiv \bar{\boldsymbol{\sigma}}_T, \tag{45}$$

i.e., a formulation in which the kinematic constraint and the static constraint are in place simultaneously, as pointed out by Carol and Bažant (1997). Linear elasticity with this specific choice of E_V, E_D and E_T seems to yield the only microplane laws that lead to a model with the double constraint. Other interesting properties of the microplane model are linked to this specific choice of the microplane elasticity moduli as well, such as being able to derive a damage tensor independently from rheology as proposed by Carol et al. (1991) or having expressions for the macroscopic stress and strain invariants in terms of the simple integrals of microplane stresses and strains.

6. Microplane damage

In this Section, we will evaluate the constitutive formulation assuming that damage is the dominating dissipative mechanism on the microplane. Following the ideas of Bažant and Prat (1988), the evolution of damage is assumed to be different for each component. Consequently, three individual damage parameters have to be introduced. Thus,

$$\boldsymbol{q} = \{d_V, d_D, d_T\} \quad \text{with } 0 \leqslant d_V, d_D, d_T \leqslant 1. \tag{46}$$

The individual damage parameters can be understood as the effective surface density of microdefects (Lemaitre, 1992), whereby d_V and d_D can be associated with the direction normal to the plane and d_T is associated to the in-plane damage. The microscopic free energy can thus be written in terms of the strain components and the damage parameters,

$$\Psi^{mic} = \hat{\Psi}^{mic}(\epsilon_V, \epsilon_D, \boldsymbol{\epsilon}_T, d_V, d_D, d_T). \tag{47}$$

As in classical continuum damage theories, the values of the damage variables grow from zero to one with increasing loading. They can be interpreted as a reduction of the corresponding elastic properties, yielding the following definition of the microscopic free energy:

$$\Psi^{mic} = [1 - d_V]W_V(\epsilon_V) + [1 - d_D]W_D(\epsilon_D) + [1 - d_T]W_T(\boldsymbol{\epsilon}_T). \tag{48}$$

Herein, W_V, W_D and W_T denote the microscopic stored energy functions according to Eq. (35). Again, the microscopic version of the Clausius–Duhem inequality yields the definition of the microscopic constitutive stresses as thermodynamically conjugate variables to the corresponding strain components. That is,

$$\begin{aligned}
\sigma_V &:= \frac{\partial \Psi^{mic}}{\partial \epsilon_V} = E_V^{ed}\epsilon_V, \qquad E_V^{ed} := [1 - d_V]E_V, \\
\sigma_D &:= \frac{\partial \Psi^{mic}}{\partial \epsilon_D} = E_D^{ed}\epsilon_D, \qquad E_D^{ed} := [1 - d_D]E_D, \\
\boldsymbol{\sigma}_T &:= \frac{\partial \Psi^{mic}}{\partial \boldsymbol{\epsilon}_T} = \boldsymbol{E}_T^{ed} \cdot \boldsymbol{\epsilon}_T, \qquad \boldsymbol{E}_T^{ed} := [1 - d_T]\boldsymbol{E}_T.
\end{aligned} \tag{49}$$

Furthermore, the microscopic dissipation inequality

$$\mathscr{D}^{mic} := Y_V \dot{d}_V + Y_D \dot{d}_D + Y_T \dot{d}_T \quad \text{with } \mathscr{D}^{mic} \geqslant 0 \tag{50}$$

renders the definitions of the energy release rates Y_V, Y_D and Y_T as the thermodynamically conjugate variables to the damage parameters,

$$Y_{\mathrm{V}} := -\frac{\partial \Psi^{\mathrm{mic}}}{\partial d_{\mathrm{V}}} = W_{\mathrm{V}}, \qquad Y_{\mathrm{D}} := -\frac{\partial \Psi^{\mathrm{mic}}}{\partial d_{\mathrm{D}}} = W_{\mathrm{D}}, \qquad Y_{\mathrm{T}} := -\frac{\partial \Psi^{\mathrm{mic}}}{\partial d_{\mathrm{T}}} = W_{\mathrm{T}}. \tag{51}$$

The damage loading functions are introduced in the following form:

$$\begin{aligned} &\Phi_{\mathrm{V}}(Y_{\mathrm{V}}, d_{\mathrm{V}}) := \phi_{\mathrm{V}}(Y_{\mathrm{V}}) - d_{\mathrm{V}} \leqslant 0, \\ &\Phi_{\mathrm{D}}(Y_{\mathrm{D}}, d_{\mathrm{D}}) := \phi_{\mathrm{D}}(Y_{\mathrm{D}}) - d_{\mathrm{D}} \leqslant 0, \\ &\Phi_{\mathrm{T}}(Y_{\mathrm{T}}, d_{\mathrm{T}}) := \phi_{\mathrm{T}}(Y_{\mathrm{T}}) - d_{\mathrm{T}} \leqslant 0. \end{aligned} \tag{52}$$

From the evaluation of the constrained optimization problem arising from the dissipation inequality (50) in combination with the postulate of maximum dissipation under the constraints (52), we gain the evolution laws for the damage parameters

$$\dot{d}_{\mathrm{V}} = \dot{\kappa}_{\mathrm{V}}\, \partial_{Y_{\mathrm{V}}} \phi_{\mathrm{V}}, \qquad \dot{d}_{\mathrm{D}} = \dot{\kappa}_{\mathrm{D}}\, \partial_{Y_{\mathrm{D}}} \phi_{\mathrm{D}}, \qquad \dot{d}_{\mathrm{T}} = \dot{\kappa}_{\mathrm{T}}\, \partial_{Y_{\mathrm{T}}} \phi_{\mathrm{T}} \tag{53}$$

as well as the Kuhn–Tucker loading–unloading conditions, i.e.

$$\begin{aligned} &\Phi_{\mathrm{V}} \leqslant 0, \;\; \dot{\kappa}_{\mathrm{V}} \geqslant 0, \quad \Phi_{\mathrm{V}}\, \dot{\kappa}_{\mathrm{V}} = 0, \\ &\Phi_{\mathrm{D}} \leqslant 0, \;\; \dot{\kappa}_{\mathrm{D}} \geqslant 0, \quad \Phi_{\mathrm{D}}\, \dot{\kappa}_{\mathrm{D}} = 0, \\ &\Phi_{\mathrm{T}} \leqslant 0, \;\; \dot{\kappa}_{\mathrm{T}} \geqslant 0, \quad \Phi_{\mathrm{T}}\, \dot{\kappa}_{\mathrm{T}} = 0. \end{aligned} \tag{54}$$

The corresponding consistency conditions can be expressed as follows:

$$\dot{\Phi}_{\mathrm{V}} \dot{\kappa}_{\mathrm{V}} = 0, \qquad \dot{\Phi}_{\mathrm{D}} \dot{\kappa}_{\mathrm{D}} = 0, \qquad \dot{\Phi}_{\mathrm{T}} \dot{\kappa}_{\mathrm{T}} = 0. \tag{55}$$

Their evaluation according to Simo and Ju (1987) yields the evolution equations for the history parameters κ_{V}, κ_{D} and κ_{T},

$$\dot{\kappa}_{\mathrm{V}} = \dot{Y}_{\mathrm{V}} \geqslant 0, \qquad \dot{\kappa}_{\mathrm{D}} = \dot{Y}_{\mathrm{D}} \geqslant 0, \qquad \dot{\kappa}_{\mathrm{T}} = \dot{Y}_{\mathrm{T}} \geqslant 0. \tag{56}$$

Consequently, the history parameters can be expressed in the following closed form:

$$\kappa_{\mathrm{V}} = \max_{-\infty < s < \tau} (Y_{\mathrm{V}}(s), \kappa_{\mathrm{V}}^0), \qquad \kappa_{\mathrm{D}} = \max_{-\infty < s < \tau} (Y_{\mathrm{D}}(s), \kappa_{\mathrm{D}}^0), \qquad \kappa_{\mathrm{T}} = \max_{-\infty < s < \tau} (Y_{\mathrm{T}}(s), \kappa_{\mathrm{T}}^0), \tag{57}$$

whereby κ_{V}^0, κ_{D}^0 and κ_{T}^0 denote individual damage threshold values. Moreover, the damage evolution laws can be simplified in the following form:

$$d_{\mathrm{V}} = \phi_{\mathrm{V}}(\kappa_{\mathrm{V}}), \qquad d_{\mathrm{D}} = \phi_{\mathrm{D}}(\kappa_{\mathrm{D}}), \qquad d_{\mathrm{T}} = \phi_{\mathrm{T}}(\kappa_{\mathrm{T}}). \tag{58}$$

Finally, the macroscopic Clausius–Duhem inequality (10) can be evaluated, yielding the macroscopic stress tensor $\boldsymbol{\sigma}$ as thermodynamically conjugate variable to the macroscopic strain tensor $\boldsymbol{\epsilon}$,

$$\boldsymbol{\sigma} = \frac{\partial \Psi^{\mathrm{mac}}}{\partial \boldsymbol{\epsilon}} = \boldsymbol{E}_{\mathrm{s}}^{\mathrm{ed}} : \boldsymbol{\epsilon}. \tag{59}$$

Herein, $\boldsymbol{E}_{\mathrm{s}}^{\mathrm{ed}}$ denotes the fourth order elasticity secant tensor modified due to damage. It can be expressed in terms of the individual elasticity moduli $E_{\mathrm{V}}^{\mathrm{ed}}$, $E_{\mathrm{D}}^{\mathrm{ed}}$ and $\boldsymbol{E}_{\mathrm{T}}^{\mathrm{ed}}$ modified due to damage and integrated over the hemisphere, i.e.

$$\boldsymbol{E}_{\mathrm{s}}^{\mathrm{ed}} = \frac{3}{2\pi} \int_{\Omega} \left[E_{\mathrm{V}}^{\mathrm{ed}} \boldsymbol{V} \otimes \boldsymbol{V} + E_{\mathrm{D}}^{\mathrm{ed}} \boldsymbol{D} \otimes \boldsymbol{D} + \boldsymbol{T}^{\mathrm{T}} \cdot \boldsymbol{E}_{\mathrm{T}}^{\mathrm{ed}} \cdot \boldsymbol{T} \right] \mathrm{d}\Omega. \tag{60}$$

The linearization of Eq. (59) yields the elasto-damage tangent operator $\boldsymbol{E}_{\mathrm{t}}^{\mathrm{ed}}$,

$$\boldsymbol{E}_{\mathrm{t}}^{\mathrm{ed}} = \boldsymbol{E}_{\mathrm{s}}^{\mathrm{ed}} - \frac{3}{2\pi} \int_{\Omega} \left[\frac{\partial \phi_{\mathrm{V}}}{\partial \kappa_{\mathrm{V}}} \frac{\sigma_{\mathrm{V}}^2}{[1 - d_{\mathrm{V}}]^2} \boldsymbol{V} \otimes \boldsymbol{V} + \frac{\partial \phi_{\mathrm{D}}}{\partial \kappa_{\mathrm{D}}} \frac{\sigma_{\mathrm{D}}^2}{[1 - d_{\mathrm{D}}]^2} \boldsymbol{D} \otimes \boldsymbol{D} + \frac{\partial \phi_{\mathrm{T}}}{\partial \kappa_{\mathrm{T}}} \boldsymbol{T}^{\mathrm{T}} \cdot \frac{\boldsymbol{\sigma}_{\mathrm{T}} \otimes \boldsymbol{\sigma}_{\mathrm{T}}}{[1 - d_{\mathrm{T}}]^2} \cdot \boldsymbol{T} \right] \mathrm{d}\Omega. \tag{61}$$

Table 1
Constitutive equations of microplane damage

Free energy	$\Psi^{\mathrm{mac}} = \hat{\Psi}^{\mathrm{mac}}(\Psi_{\mathrm{V}}, \Psi_{\mathrm{D}}, \Psi_{\mathrm{T}}) = \frac{3}{2\pi}\int_{\Omega}\left[\Psi_{\mathrm{V}}^{\mathrm{mic}} + \Psi_{\mathrm{D}}^{\mathrm{mic}} + \Psi_{\mathrm{T}}^{\mathrm{mic}}\right]\mathrm{d}\Omega$
Volumetric	$\Psi_{\mathrm{V}}^{\mathrm{mic}} = \hat{\Psi}_{\mathrm{V}}^{\mathrm{mic}}(\epsilon_{\mathrm{V}}, d_{\mathrm{V}}) = [1-d_{\mathrm{V}}]\, W_{\mathrm{V}}$
Deviatoric	$\Psi_{\mathrm{D}}^{\mathrm{mic}} = \hat{\Psi}_{\mathrm{D}}^{\mathrm{mic}}(\epsilon_{\mathrm{D}}, d_{\mathrm{D}}) = [1-d_{\mathrm{D}}]\, W_{\mathrm{D}}$
Tangential	$\Psi_{\mathrm{T}}^{\mathrm{mic}} = \hat{\Psi}_{\mathrm{T}}^{\mathrm{mic}}(\boldsymbol{\epsilon}_{\mathrm{T}}, d_{\mathrm{T}}) = [1-d_{\mathrm{T}}]\, W_{\mathrm{T}}$
Stresses	$\boldsymbol{\sigma} = \partial\Psi^{\mathrm{mac}}/\partial\boldsymbol{\epsilon} = \frac{3}{2\pi}\int_{\Omega}\left[\boldsymbol{V}\sigma_{\mathrm{V}} + \boldsymbol{D}\sigma_{\mathrm{D}} + \boldsymbol{T}^{\mathrm{T}}\cdot\boldsymbol{\sigma}_{\mathrm{T}}\right]\mathrm{d}\Omega$
Volumetric	$\sigma_{\mathrm{V}} = \partial\Psi^{\mathrm{mic}}/\partial\epsilon_{\mathrm{V}} = [1-d_{\mathrm{V}}]\, E_{\mathrm{V}}\epsilon_{\mathrm{V}}$
Deviatoric	$\sigma_{\mathrm{D}} = \partial\Psi^{\mathrm{mic}}/\partial\epsilon_{\mathrm{D}} = [1-d_{\mathrm{D}}]\, E_{\mathrm{D}}\epsilon_{\mathrm{D}}$
Tangential	$\boldsymbol{\sigma}_{\mathrm{T}} = \partial\Psi^{\mathrm{mic}}/\partial\boldsymbol{\epsilon}_{\mathrm{T}} = [1-d_{\mathrm{T}}]\, \boldsymbol{E}_{\mathrm{T}}\cdot\boldsymbol{\epsilon}_{\mathrm{T}}$
Energy release rates	
Volumetric	$Y_{\mathrm{V}} = -\partial\Psi^{\mathrm{mic}}/\partial d_{\mathrm{V}} = W_{\mathrm{V}}$
Deviatoric	$Y_{\mathrm{D}} = -\partial\Psi^{\mathrm{mic}}/\partial d_{\mathrm{D}} = W_{\mathrm{D}}$
Tangential	$Y_{\mathrm{T}} = -\partial\Psi^{\mathrm{mic}}/\partial d_{\mathrm{T}} = W_{\mathrm{T}}$
Loading functions	
Volumetric	$\Phi_{\mathrm{V}} = \phi_{\mathrm{V}}(Y_{\mathrm{V}}) - d_{\mathrm{V}} \leqslant 0$
Deviatoric	$\Phi_{\mathrm{D}} = \phi_{\mathrm{D}}(Y_{\mathrm{D}}) - d_{\mathrm{D}} \leqslant 0$
Tangential	$\Phi_{\mathrm{T}} = \phi_{\mathrm{T}}(Y_{\mathrm{T}}) - d_{\mathrm{T}} \leqslant 0$
Kuhn–Tucker conditions	
Volumetric	$\dot{\kappa}_{\mathrm{V}} \geqslant 0 \quad \Phi_{\mathrm{V}} \leqslant 0 \quad \dot{\kappa}_{\mathrm{V}}\,\Phi_{\mathrm{V}} = 0 \quad \dot{\kappa}_{\mathrm{V}}\,\dot{\Phi}_{\mathrm{V}} = 0$
Deviatoric	$\dot{\kappa}_{\mathrm{D}} \geqslant 0 \quad \Phi_{\mathrm{D}} \leqslant 0 \quad \dot{\kappa}_{\mathrm{D}}\,\Phi_{\mathrm{D}} = 0 \quad \dot{\kappa}_{\mathrm{D}}\,\dot{\Phi}_{\mathrm{D}} = 0$
Tangential	$\dot{\kappa}_{\mathrm{T}} \geqslant 0 \quad \Phi_{\mathrm{T}} \leqslant 0 \quad \dot{\kappa}_{\mathrm{T}}\,\Phi_{\mathrm{T}} = 0 \quad \dot{\kappa}_{\mathrm{T}}\,\dot{\Phi}_{\mathrm{T}} = 0$
Evolution laws	
Volumetric	$\dot{d}_{\mathrm{V}} = \dot{\kappa}_{\mathrm{V}}\,\partial_{Y_{\mathrm{V}}}\phi_{\mathrm{V}} \quad \dot{\kappa}_{\mathrm{V}} = \dot{Y}_{\mathrm{V}}$
Deviatoric	$\dot{d}_{\mathrm{D}} = \dot{\kappa}_{\mathrm{D}}\,\partial_{Y_{\mathrm{D}}}\phi_{\mathrm{D}} \quad \dot{\kappa}_{\mathrm{D}} = \dot{Y}_{\mathrm{D}}$
Tangential	$\dot{d}_{\mathrm{T}} = \dot{\kappa}_{\mathrm{T}}\,\partial_{Y_{\mathrm{T}}}\phi_{\mathrm{T}} \quad \dot{\kappa}_{\mathrm{T}} = \dot{Y}_{\mathrm{T}}$

The macroscopic dissipation inequality $\mathscr{D}^{\mathrm{mac}} \geqslant 0$ is guaranteed, since the microscopic dissipation inequality is fulfilled in accordance with Eq. (50). The constitutive equations of microplane damage are summarized in Table 1.

Remark: According to the original microplane models proposed by Bažant and coworkers, we have introduced independent damage variables for the volumetric, the deviatoric and the tangential behavior. If, in contrast to this, only one damage variable d is introduced, the microscopic free energy is given as follows:

$$\Psi^{\mathrm{mic}} = \hat{\Psi}^{\mathrm{mic}}(\epsilon_{\mathrm{V}}, \epsilon_{\mathrm{D}}, \boldsymbol{\epsilon}_{\mathrm{T}}, d) = [1-d]\,[W_{\mathrm{V}}(\epsilon_{\mathrm{V}}) + W_{\mathrm{D}}(\epsilon_{\mathrm{D}}) + W_{\mathrm{T}}(\boldsymbol{\epsilon}_{\mathrm{T}})]. \tag{62}$$

Moreover, we can define a damage-loading function of the following form:

$$\Phi := \phi(Y) - d \leqslant 0 \quad \text{with } Y := W_{\mathrm{V}}(\epsilon_{\mathrm{V}}) + W_{\mathrm{D}}(\epsilon_{\mathrm{D}}) + W_{\mathrm{T}}(\boldsymbol{\epsilon}_{\mathrm{T}}). \tag{63}$$

With the argumentation of Simo and Ju (1987) and the evaluation of the macroscopic constitutive equations as described in Section 3, we obtain the following definition of the macroscopic stress tensor $\boldsymbol{\sigma}$:

$$\boldsymbol{\sigma} = \boldsymbol{E}_{\mathrm{s}}^{\mathrm{ed}} : \boldsymbol{\epsilon} \quad \text{with } \boldsymbol{E}_{\mathrm{s}}^{\mathrm{ed}} = \frac{3}{2\pi}\int_{\Omega}[1-d]\left[E_{\mathrm{V}}\boldsymbol{V}\otimes\boldsymbol{V} + E_{\mathrm{D}}\boldsymbol{D}\otimes\boldsymbol{D} + \boldsymbol{T}^{\mathrm{T}}\cdot\boldsymbol{E}_{\mathrm{T}}\cdot\boldsymbol{T}\right]\mathrm{d}\Omega. \tag{64}$$

The elasto-damage tangent operator for the microplane damage formulation in terms of only one damage variable is then given as follows:

$$\boldsymbol{E}_{\mathrm{t}}^{\mathrm{ed}} = \boldsymbol{E}_{\mathrm{s}}^{\mathrm{ed}} - \frac{3}{2\pi}\int_{\Omega}\frac{\partial\phi}{\partial\kappa}\left[\boldsymbol{V}\sigma_{\mathrm{V}} + \boldsymbol{D}\sigma_{\mathrm{D}} + \boldsymbol{T}^{\mathrm{T}}\cdot\boldsymbol{\sigma}_{\mathrm{T}}\right]\otimes[\sigma_{\mathrm{V}}\boldsymbol{V} + \sigma_{\mathrm{D}}\boldsymbol{D} + \boldsymbol{\sigma}_{\mathrm{T}}\cdot\boldsymbol{T}]/[1-d]^2\,\mathrm{d}\Omega. \tag{65}$$

7. Microplane plasticity

We will now establish the situation for which plastic sliding is the dominant dissipative mechanism on the microplane. Based on the assumption of small strains, the macroscopic strain tensor can be additively decomposed into an elastic and a plastic part,

$$\boldsymbol{\epsilon} := \boldsymbol{\epsilon}^{\mathrm{e}} + \boldsymbol{\epsilon}^{\mathrm{p}}. \tag{66}$$

Consequently, according to the kinematic constraint, the microplane strain components can be expressed by the same additive decomposition,

$$\epsilon_{\mathrm{V}} := \epsilon_{\mathrm{V}}^{\mathrm{e}} + \epsilon_{\mathrm{V}}^{\mathrm{p}}, \qquad \epsilon_{\mathrm{D}} := \epsilon_{\mathrm{D}}^{\mathrm{e}} + \epsilon_{\mathrm{D}}^{\mathrm{p}}, \qquad \boldsymbol{\epsilon}_{\mathrm{T}} := \boldsymbol{\epsilon}_{\mathrm{T}}^{\mathrm{e}} + \boldsymbol{\epsilon}_{\mathrm{T}}^{\mathrm{p}}. \tag{67}$$

In the most general form, the vector of internal variables $\boldsymbol{q}$ consists of the three plastic strain components $\epsilon_{\mathrm{V}}^{\mathrm{p}}$, $\epsilon_{\mathrm{D}}^{\mathrm{p}}$ and $\boldsymbol{\epsilon}_{\mathrm{T}}^{\mathrm{p}}$ and a set of internal variables $\boldsymbol{\kappa}$, describing the hardening behavior. For sake of transparency, we will assume that the influence of kinematic hardening is negligible. We thus introduce one single hardening variable κ for each plane, describing the isotropic hardening behavior,

$$\boldsymbol{q} = \{\epsilon_{\mathrm{V}}^{\mathrm{p}}, \epsilon_{\mathrm{D}}^{\mathrm{p}}, \boldsymbol{\epsilon}_{\mathrm{T}}^{\mathrm{p}}, \kappa\}. \tag{68}$$

Accordingly, the microscopic free energy can be defined in terms of the total strains, the plastic strains and the hardening variable,

$$\Psi^{\mathrm{mic}} = \hat{\Psi}^{\mathrm{mic}}\,(\epsilon_{\mathrm{V}}, \epsilon_{\mathrm{D}}, \boldsymbol{\epsilon}_{\mathrm{T}}, \epsilon_{\mathrm{V}}^{\mathrm{p}}, \epsilon_{\mathrm{D}}^{\mathrm{p}}, \boldsymbol{\epsilon}_{\mathrm{T}}^{\mathrm{p}}, \kappa). \tag{69}$$

Based on the definition of the elastic free energy given by Eq. (34), the free energy for microplane plasticity can be expressed as follows:

$$\Psi^{\mathrm{mic}} = W_{\mathrm{V}}(\epsilon_{\mathrm{V}} - \epsilon_{\mathrm{V}}^{\mathrm{p}}) + W_{\mathrm{D}}(\epsilon_{\mathrm{D}} - \epsilon_{\mathrm{D}}^{\mathrm{p}}) + W_{\mathrm{T}}(\boldsymbol{\epsilon}_{\mathrm{T}} - \boldsymbol{\epsilon}_{\mathrm{T}}^{\mathrm{p}}) + \int_0^{\kappa} \phi(\kappa)\mathrm{d}\hat{\kappa}. \tag{70}$$

Again, W_{V}, W_{D} and W_{T} define the microscopic stored energy functions according to Eq. (35). The additional term $\int_0^{\kappa} \phi(\kappa)\mathrm{d}\hat{\kappa}$ accounts for the isotropic hardening behavior. By evaluating the microscopic Clausius–Duhem inequality, we obtain the definition of the microscopic constitutive stresses as thermodynamically conjugate values to the elastic strains, i.e.

$$\sigma_{\mathrm{V}} := \frac{\partial \Psi^{\mathrm{mic}}}{\partial \epsilon_{\mathrm{V}}} = E_{\mathrm{V}}\epsilon_{\mathrm{V}}^{\mathrm{e}}, \qquad \sigma_{\mathrm{D}} := \frac{\partial \Psi^{\mathrm{mic}}}{\partial \epsilon_{\mathrm{D}}} = E_{\mathrm{D}}\epsilon_{\mathrm{D}}^{\mathrm{e}}, \qquad \boldsymbol{\sigma}_{\mathrm{T}} := \frac{\partial \Psi^{\mathrm{mic}}}{\partial \boldsymbol{\epsilon}_{\mathrm{T}}} = \boldsymbol{E}_{\mathrm{T}} \cdot \boldsymbol{\epsilon}_{\mathrm{T}}^{\mathrm{e}}. \tag{71}$$

Moreover, the microscopic dissipation inequality poses the following restrictions on the evolution of the plastic strains and the internal variable:

$$\mathscr{D}^{\mathrm{mic}} := \sigma_{\mathrm{V}}\dot{\epsilon}_{\mathrm{V}}^{\mathrm{p}} + \sigma_{\mathrm{D}}\dot{\epsilon}_{\mathrm{D}}^{\mathrm{p}} + \boldsymbol{\sigma}_{\mathrm{T}} \cdot \dot{\boldsymbol{\epsilon}}_{\mathrm{T}}^{\mathrm{p}} - \phi\dot{\kappa} \quad \text{with } \mathscr{D}^{\mathrm{mic}} \geqslant 0. \tag{72}$$

The yield function Φ can be introduced in terms of the equivalent stress φ and the yield stress ϕ,

$$\Phi = \varphi(\sigma_{\mathrm{V}}, \sigma_{\mathrm{D}}, \boldsymbol{\sigma}_{\mathrm{T}}) - \phi(\kappa) \leqslant 0, \tag{73}$$

whereby the equivalent stress φ is a function of the individual microscopic constitutive stresses, with

$$v_{\mathrm{V}} := \frac{\partial \varphi}{\partial \sigma_{\mathrm{V}}}, \qquad v_{\mathrm{D}} := \frac{\partial \varphi}{\partial \sigma_{\mathrm{D}}}, \qquad \boldsymbol{v}_{\mathrm{T}} := \frac{\partial \varphi}{\partial \boldsymbol{\sigma}_{\mathrm{T}}}. \tag{74}$$

By solving the constrained optimization problem arising from the dissipation inequality (73) in combination with the postulate of maximum dissipation under constraint (73), we obtain the following evolution equations for the plastic strains and the internal variable κ:

$$\dot{\epsilon}_{\mathrm{V}}^{\mathrm{p}} = \dot{\gamma} v_{\mathrm{V}}, \qquad \dot{\epsilon}_{\mathrm{D}}^{\mathrm{p}} = \dot{\gamma} v_{\mathrm{D}}, \qquad \dot{\boldsymbol{\epsilon}}_{\mathrm{T}}^{\mathrm{p}} = \dot{\gamma} \boldsymbol{v}_{\mathrm{T}}, \qquad \dot{\kappa} = \dot{\gamma}. \tag{75}$$

Furthermore, the Kuhn–Tucker loading unloading conditions and the consistency condition are expressed as follows:

$$\Phi \leqslant 0, \qquad \dot{\gamma} \geqslant 0, \qquad \Phi\dot{\gamma} = 0, \qquad \dot{\Phi}\dot{\gamma} = 0. \tag{76}$$

The evolution of the yield stress renders hardening modulus H,

$$\dot{\phi} = H\dot{\kappa} \quad \text{with } H = \frac{\partial\phi}{\partial\kappa}. \tag{77}$$

This formulation corresponds to a Koiter type hardening. Note that this class of hardening laws does not account for an interaction of the hardening behavior of the different microplanes. In the context of crystal plasticity, however, this interaction introduced through latent-hardening terms, cannot be neglected, since its influence is nearly of the same order as the influence of the self-hardening term considered here. The different types of hardening laws are discussed in detail by Asaro (1983).

The evaluation of the consistency condition (76) (fourth equation) yields the definition for the plastic multiplier $\dot{\gamma}$,

$$\dot{\gamma} = \tfrac{1}{h}[v_{\mathrm{V}}E_{\mathrm{V}}\boldsymbol{V} + v_{\mathrm{D}}E_{\mathrm{D}}\boldsymbol{D} + \boldsymbol{v}_{\mathrm{T}} \cdot \boldsymbol{E}_{\mathrm{T}} \cdot \boldsymbol{T}] : \dot{\boldsymbol{\epsilon}} \tag{78}$$

with

$$h := v_{\mathrm{V}}E_{\mathrm{V}}v_{\mathrm{V}} + v_{\mathrm{D}}E_{\mathrm{D}}v + \boldsymbol{v}_{\mathrm{T}} \cdot \boldsymbol{E}_{\mathrm{T}} \cdot \boldsymbol{v}_{\mathrm{T}} + H. \tag{79}$$

Consequently, we obtain the following expression for the elasto-plastic tangent operator $\boldsymbol{E}^{\mathrm{ep}}$

$$\dot{\boldsymbol{\sigma}} = \boldsymbol{E}^{\mathrm{ep}}_{\mathrm{t}} : \dot{\boldsymbol{\epsilon}} \tag{80}$$

with

$$\boldsymbol{E}^{\mathrm{ep}}_{\mathrm{t}} = \boldsymbol{E}^{\mathrm{el}} - \frac{3}{2\pi}\int_{\Omega}\frac{1}{h}\left[\boldsymbol{V}E_{\mathrm{V}}v_{\mathrm{V}} + \boldsymbol{D}E_{\mathrm{D}}v_{\mathrm{D}} + \boldsymbol{T}^{\mathrm{T}} \cdot \boldsymbol{E}_{\mathrm{T}} \cdot v_{\mathrm{T}}\right] \otimes \left[v_{\mathrm{V}}\,E_{\mathrm{V}}\boldsymbol{V} + v_{\mathrm{D}}E_{\mathrm{D}}\boldsymbol{D} + v_{\mathrm{T}} \cdot \boldsymbol{E}_{\mathrm{T}} \cdot \boldsymbol{T}\right]\mathrm{d}\Omega. \tag{81}$$

Remarkably, the structure of the elasto-plastic tangent operator is very similar to the elasto-damage tangent operator for the formulation with only one damage variable defined in Eq. (65). The constitutive equations of microplane plasticity are summarized in Table 2.

Table 2
Constitutive equations of microplane plasticity

Free energy	$\Psi^{\mathrm{mac}} = \hat{\Psi}^{\mathrm{mac}}(\Psi^{\mathrm{mic}}) = (3/2\pi)\int_{\Omega}\Psi^{\mathrm{mic}}\,\mathrm{d}\Omega$
Microscopic	$\Psi^{\mathrm{mic}} = W_{\mathrm{V}}(\epsilon^{\mathrm{e}}_{\mathrm{V}}) + W_{\mathrm{D}}(\epsilon^{\mathrm{e}}_{\mathrm{D}}) + W_{\mathrm{T}}(\boldsymbol{\epsilon}^{\mathrm{e}}_{\mathrm{T}}) + \int_0^{\kappa}\phi\,\mathrm{d}\hat{\kappa}$
Stresses	$\boldsymbol{\sigma} = \partial\Psi^{\mathrm{mac}}/\partial\boldsymbol{\epsilon} = (3/2\pi)\int_{\Omega}\left[\boldsymbol{V}\sigma_{\mathrm{V}} + \boldsymbol{D}\sigma_{\mathrm{D}} + \boldsymbol{T}^{\mathrm{T}} \cdot \boldsymbol{\sigma}_{\mathrm{T}}\right]\mathrm{d}\Omega$
Volumetric	$\sigma_{\mathrm{V}} = \partial\Psi^{\mathrm{mic}}/\partial\epsilon_{\mathrm{V}} = E_{\mathrm{V}}\epsilon^{\mathrm{e}}_{\mathrm{V}}$
Deviatoric	$\sigma_{\mathrm{D}} = \partial\Psi^{\mathrm{mic}}/\partial\epsilon_{\mathrm{D}} = E_{\mathrm{D}}\epsilon^{\mathrm{e}}_{\mathrm{D}}$
Tangential	$\boldsymbol{\sigma}_{\mathrm{T}} = \partial\Psi^{\mathrm{mic}}/\partial\boldsymbol{\epsilon}_{\mathrm{T}} = \boldsymbol{E}_{\mathrm{T}} \cdot \boldsymbol{\epsilon}^{\mathrm{e}}_{\mathrm{T}}$
Yield stress	$\phi = \partial\Psi^{\mathrm{mic}}/\partial\kappa \quad \dot{\phi} = H\dot{\kappa}$
Loading function	$\Phi = \varphi(\sigma_{\mathrm{V}}, \sigma_{\mathrm{D}}, \boldsymbol{\sigma}_{\mathrm{T}}) - \phi(\kappa) \leqslant 0$
Kuhn–Tucker conditions	$\dot{\gamma} \geqslant 0 \quad \Phi \leqslant 0 \quad \dot{\gamma}\Phi = 0 \quad \dot{\gamma}\dot{\Phi} = 0$
Evolution law	$\dot{\kappa} = \dot{\gamma}$
Plastic strains	
Volumetric	$\dot{\epsilon}^{\mathrm{p}}_{\mathrm{V}} = \dot{\gamma}\,\partial\phi_{\mathrm{V}}/\partial\sigma_{\mathrm{V}}$
Deviatoric	$\dot{\epsilon}^{\mathrm{p}}_{\mathrm{D}} = \dot{\gamma}\,\partial\phi_{\mathrm{D}}/\partial\sigma_{\mathrm{D}}$
Tangential	$\dot{\boldsymbol{\epsilon}}^{\mathrm{p}}_{\mathrm{T}} = \dot{\gamma}\,\partial\phi_{\mathrm{T}}/\partial\boldsymbol{\sigma}_{\mathrm{T}}$

8. Examples

In the following, we will investigate the spatial distribution of the material properties for the model problem of "uniaxial tension" and "simple shear" under plane strain conditions. The elastic microplane moduli are chosen in accordance with Section 5 such that the overall Young's modulus is equal to $E = 30000\ \mathrm{N\,mm^{-2}}$ and Poisson's ratio takes a value of $\nu = 0.2$. Consequently, the volumetric modulus is equal to $E_{\mathrm{V}} = 50000\ \mathrm{N\,mm^{-2}}$ according to Eq. (44). We assume that for the case of microplane damage, the deviatoric and the tangential microplane moduli are weighted equally ($E_{\mathrm{D}} = 25000\ \mathrm{N\,mm^{-2}}$ and $E_{\mathrm{T}} = 25000\ \mathrm{N\,mm^{-2}}$), whereas for the examples of microplane plasticity, we will set the deviatoric modulus equal to zero ($E_{\mathrm{D}} = 0\ \mathrm{N\,mm^{-2}}$ and $E_{\mathrm{T}} = 41667\ \mathrm{N\,mm^{-2}}$). For the uniaxial tension test as well as for the simple shear problem, a plane strain situation is assumed.

8.1. Microplane elasticity

First, the spatial distribution of the driving forces for microplane damage and microplane plasticity will be elaborated assuming an initially elastic material behavior. Fig. 3(a)–(c) depict the distribution of the driving forces for microplane damage, the microscopic stored energy components

$$W_{\mathrm{V}} = \tfrac{1}{2}\epsilon_{\mathrm{V}} E_{\mathrm{V}} \epsilon_{\mathrm{V}}, \qquad W_{\mathrm{D}} = \tfrac{1}{2}\epsilon_{\mathrm{D}} E_{\mathrm{D}} \epsilon_{\mathrm{D}}, \qquad W_{\mathrm{T}} = \tfrac{1}{2}\boldsymbol{\epsilon}_{\mathrm{T}} \cdot \boldsymbol{E}_{\mathrm{V}} \cdot \boldsymbol{\epsilon}_{\mathrm{T}} \tag{82}$$

for the case of uniaxial tension. For the analysis, the numerical integration over the hemisphere has been performed with $n_{\mathrm{mp}} = 21$ microplanes. In contrast to the microscopic volumetric stored energy depicted in Fig. 3(a), the microscopic deviatoric and tangential stored energies of Fig. 3(b) and (c) are not distributed uniformly in space. Fig. 3(d) shows the distribution of the equivalent stress φ as driving force for microplane plasticity. For sake of transparency, we will assume that the equivalent stress is independent of the hydrostatic pressure, such that

$$\varphi(\sigma_{\mathrm{V}}, \sigma_{\mathrm{D}}, \boldsymbol{\sigma}_{\mathrm{T}}) = \sqrt{[\boldsymbol{\sigma}_{\mathrm{T}} \cdot \boldsymbol{\sigma}_{\mathrm{T}}]}. \tag{83}$$

Fig. 4 depict the distribution of the microscopic stored energy components and the equivalent stress for the model example of simple shear. Obviously, the results strongly depend on the type of loading. Conse-

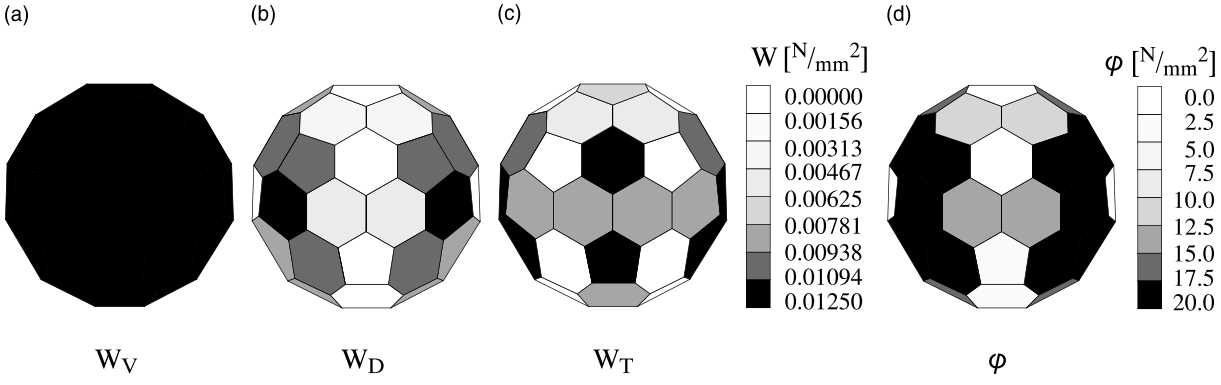

Fig. 3. Uniaxial tension – elastic microplane properties.

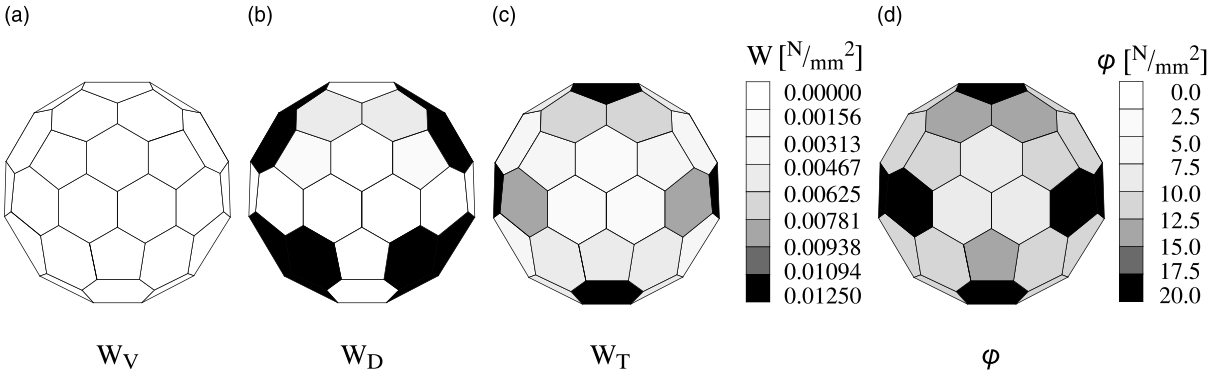

Fig. 4. Simple shear – elastic microplane properties.

quently, a completely different distribution of the elastic properties can be observed for the two different loading situations. For example, the tangential energy W_T for the simple shear test (Fig. 4(c)) takes maximum values at the upper, the lower, the left and the right microplane, whereas for the uniaxial tension test (Fig. 3(c)), these microplanes exhibit no tangential straining at all. Note that for the case of simple shear, the volumetric stored energy is equal to zero since for that type of loading all strain components except for the shear strain ϵ_{12} are equal to zero.

8.2. Microplane damage

The subsequent analysis is based on a damage formulation with three different damage moduli as derived in Section 6. The evolution of the damage moduli is assumed to be of an exponential type with

$$d(\kappa) = 1 - \exp\left[-\left[\frac{\kappa}{a}\right]^p\right]. \tag{84}$$

Accordingly, two additional parameters are introduced for each component. They are chosen as $a_V = 0.009$, $p_V = 0.5$, $a_D = 0.0125$, $p_D = 0.4$, $a_T = 0.032$ and $p_T = 0.5$, respectively. The load–displacement curves for the uniaxial tension as well as for the simple shear example are depicted in Fig. 5. Figs. 6 and 7 show the spatial development of the deviatoric and the tangential damage variable for the uniaxial tension test. Each series of four figures corresponds to the load steps indicated in the load–displacement diagram.

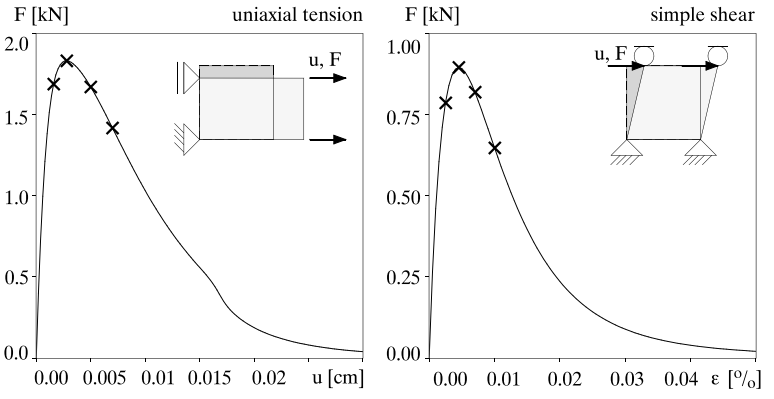

Fig. 5. Load–displacement curves for microplane damage.

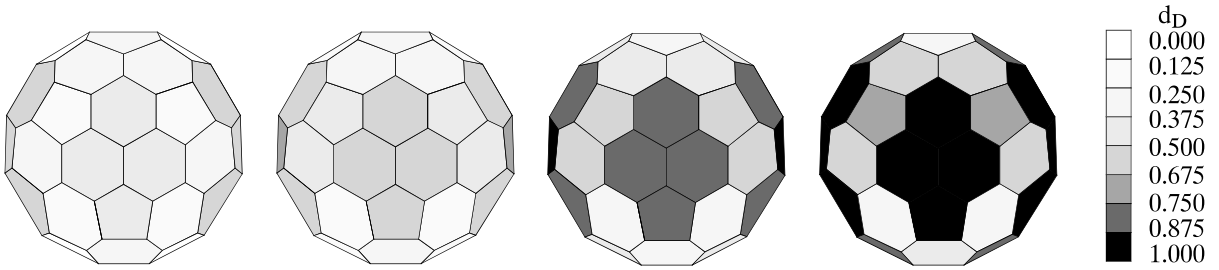

Fig. 6. Uniaxial tension – evolution of deviatoric damage d_D.

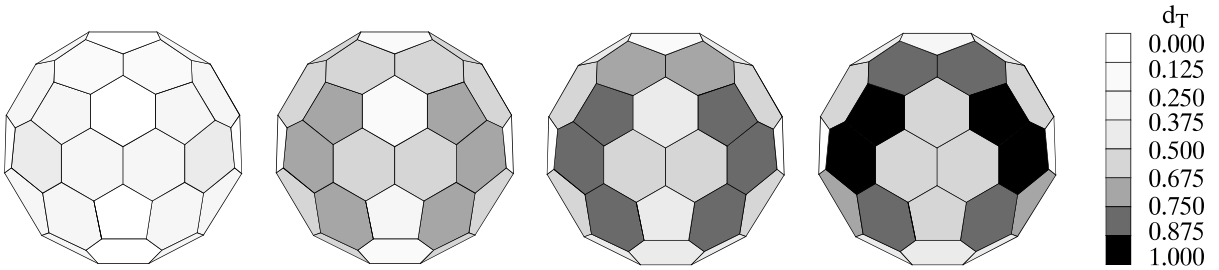

Fig. 7. Uniaxial tension – evolution of tangential damage d_T.

During the loading history, the formation of specific distribution patterns can be observed. Deviatoric damage, for example, takes maximum values in the left and right microplane which are situated normal to the loading axis, compare Fig. 6. The tangential damage variable depicted in Fig. 7 takes a distribution which is almost inverse to the one of deviatoric damage. The development of the spatial distribution of the damage moduli for the simple shear test is given in Figs. 8 and 9. The same tendencies towards a loading specific texture evolution can be observed.

The final distribution of the microscopic energies at the end of the loading history can give further insight into the loading mechanisms taking place on the microplanes. The microscopic energies W_D and W_T for the two different loading scenarios are shown in Fig. 10(a)–(d). Different strain patterns have developed under the different loading situations. Furthermore, the distinct textures can be understood as a result of various loading and unloading situations on the different microplanes. As soon as the mostly loaded microplanes locally enter the softening regime, the strains tend to concentrate in only a few microplanes whereas other microplanes exhibit unloading. This phenomenon of "microscopic localization" is characteristic for microplane based models. It represents an additional microscopic instability, which is superposed to the macroscopic instability caused by an overall softening behavior. However, the microscopic localization can take place long before the overall ultimate load is reached. If too many microplanes unload simultaneously, the undefined loading situation might even lead to a loss of convergence of the overall calculation.

8.3. Microplane plasticity

Microplane plasticity will be analyzed for the loading function introduced in Section 8.1. For sake of simplicity, we will assume a linear softening relation defined by the following relation

$$\phi(\kappa) = \sigma_Y + H\kappa \tag{85}$$

with the initial yield stress of $\sigma_Y = 50\ \mathrm{N\,mm^{-2}}$ and a softening modulus $H = -2000\ \mathrm{N\,mm^{-2}}$. The load–displacement diagrams corresponding to the two loading cases are depicted in Fig. 11. The development of

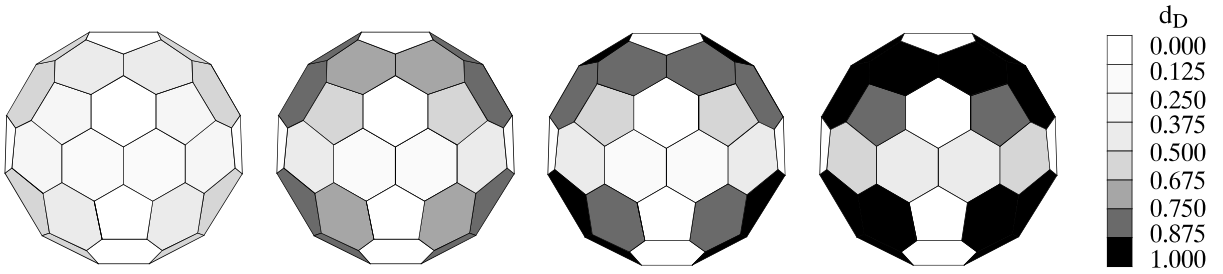

Fig. 8. Simple shear – evolution of deviatoric damage d_D.

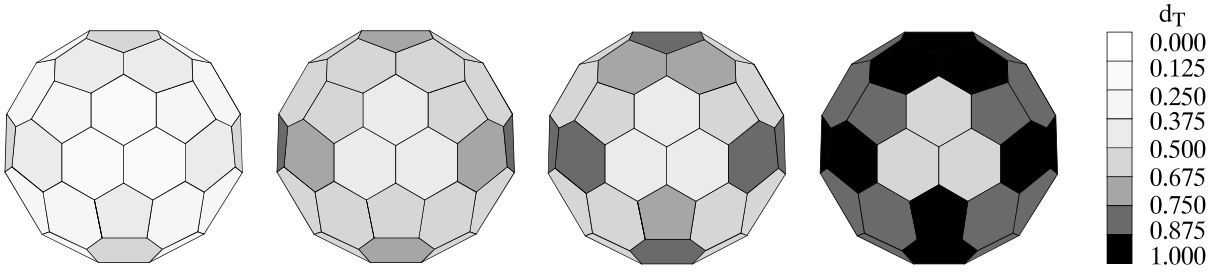

Fig. 9. Simple shear – evolution of tangential damage d_T.

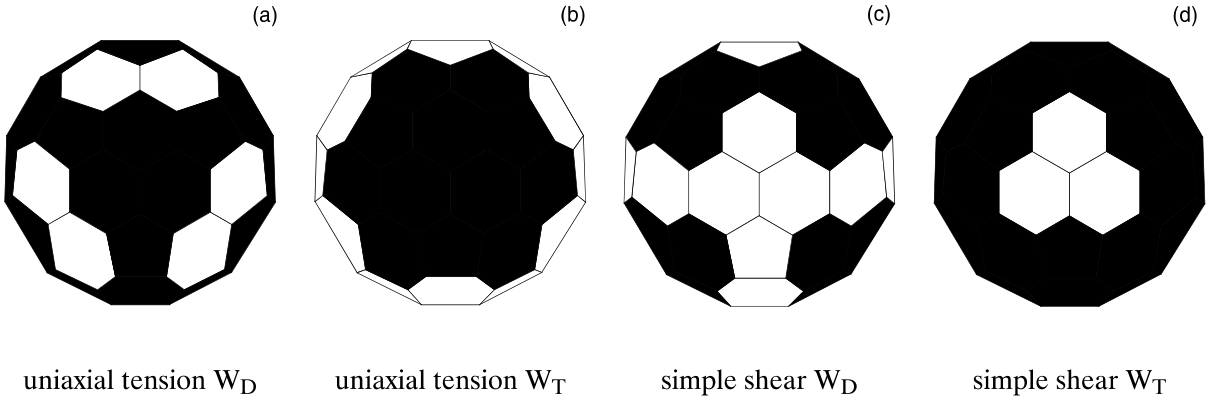

Fig. 10. Energy distribution at final state of loading.

the distribution of the plastic multiplier γ for the uniaxial tension and the simple shear case is demonstrated in Figs. 12 and 13. Again, a tendency towards texture evolution can be observed. Under uniaxial tension, the plastic strains tend to concentrate in the planes situated under an angle of about 45° towards the loading axis in the loading plane. For the simple shear case, however, plastic straining takes maximum values in the upper, lower, left and right microplane. Nevertheless, the texture evolution for this particular example of microplane plasticity seems to be less pronounced than in the previous example of microplane damage. The loading situation is defined in a much stricter sense, since only one loading function was introduced in contrast to the microplane damage model. Consequently, microscopic unloading and reloading does not take place as frequently as in the previous example.

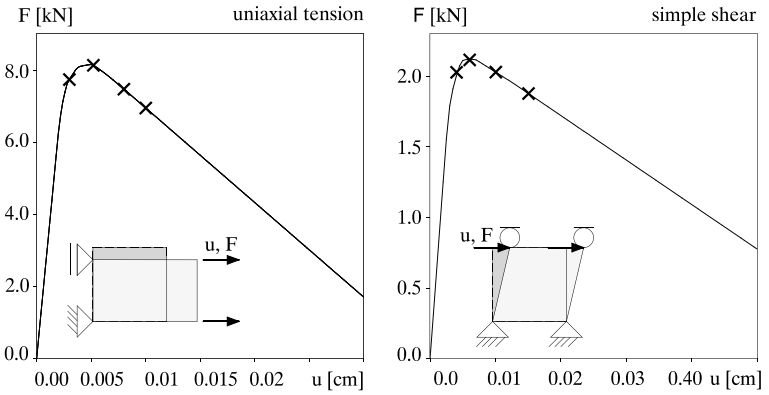

Fig. 11. Load–displacement curves for microplane plasticity.

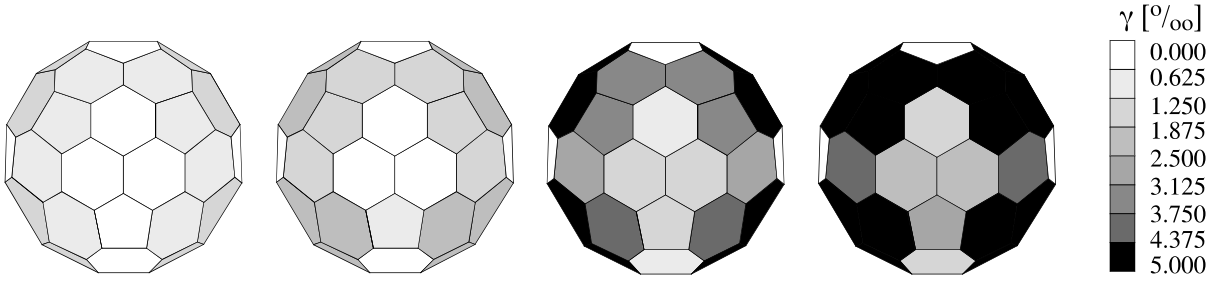

Fig. 12. Uniaxial tension – evolution of plastic multiplier γ.

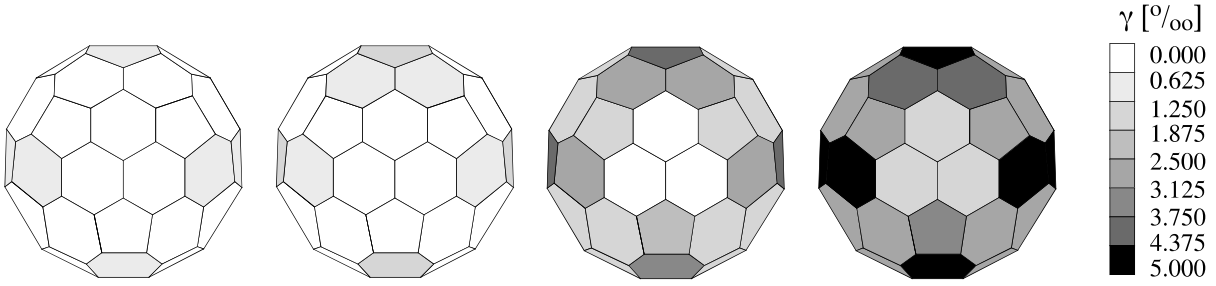

Fig. 13. Simple shear – evolution of plastic multiplier γ.

9. Conclusion

It has been the primary objective of this contribution to provide a general, thermodynamically consistent approach to derive constitutive laws within the concept of the microplane theory. Thereby, we aimed at a formulation which allows for the description of arbitrary material behavior at the micro and macroscales. The main assumption for these developments was the postulate of microscopic free energies on the individual microplanes, which could be related to the macroscopic free energy in an integral sense as was

proposed in the companion Part I to this paper. A main theoretical result is that macroscopic dissipation may be expressed as the integral of dissipation on each microplane. Thereby, the microplane constitutive laws were chosen such that the energy dissipation on each plane is guaranteed to be non-negative. Consequently, the second principle of thermodynamics is automatically satisfied for the macroscopic equations. Likewise, the corresponding macroscopic constitutive relations followed by integration over the hemisphere.

As an illustration, the generic concept has been applied to model elasticity, elasto-damage and elasto-plasticity. The results have been investigated for the examples of pointwise uniaxial tension and simple shear. Thereby, we analyzed the pointwise texture evolution or rather microscopic localization on the activated microplanes. In summary, we believe that this contribution clarified issues of how to formulate in a straightforward and thermodynamically admissible way a wide class of microplane based constitutive models.

Acknowledgements

Partial support from DGICYT-MEC (Madrid, Spain) through grant PB96-0500 to the third author is gratefully acknowledged.

Appendix A

In Section 5, an isotropic material behavior was assumed such that the integral expression of Eq. (11) could be evaluated analytically. For the general anisotropic material behavior, however, this analytical evaluation becomes nearly impossible. The integral expressions resulting from the constitutive equations can be evaluated by applying a numerical quadrature technique. The integral over all possible directions in space is thus replaced by a weighted sum of the integrand evaluated at a finite number n_{mp} of discrete directions. In the context of the microplane theory, each of these directions can be associated with one microplane on which the planewise constitutive laws are evaluated. The numerical integration will be demonstrated for the macroscopic stress tensor $\boldsymbol{\sigma}$ as a typical representative of the integral structures. Its definition based on the general definition of the overall stress tensor (17) can thus be approximated as follows:

$$\boldsymbol{\sigma} \approx \sum_{I=1}^{n_{\mathrm{mp}}} \left[\boldsymbol{V}^I \frac{\partial \Psi^{\mathrm{mic}\,I}}{\partial \epsilon_{\mathrm{V}}^I} + \boldsymbol{D}^I \frac{\partial \Psi^{\mathrm{mic}\,I}}{\partial \epsilon_{\mathrm{D}}^I} + \boldsymbol{T}^{\mathrm{T}I} \cdot \frac{\partial \Psi^{\mathrm{mic}\,I}}{\partial \boldsymbol{\epsilon}_{\mathrm{T}}^I} \right] w^I.$$

Herein, $\Psi^{\mathrm{mic}\,I}$ is the microscopic free energy associated with the Ith material direction and w^I are the corresponding weight coefficients. Furthermore, ϵ_{V}^I, ϵ_{D}^I and $\boldsymbol{\epsilon}_{\mathrm{T}}^I$ denote the strain components of the Ith plane and $\boldsymbol{V}^I$, $\boldsymbol{D}^I$ and $\boldsymbol{T}^I$ are the related projection tensors which can be expressed in terms of the plane's normal $\boldsymbol{n}^I$. Accordingly, the definitions of the other integral structures can be evaluated in an analogous fashion.

The number of microplanes n_{mp} determines the order of accuracy of the approximation. Bažant and Oh (1985, 1986) have analyzed several integration techniques based on a mathematical analysis by Stroud (1971). According to their experience, 42 microplanes yield a sufficiently accurate approximation. Due to symmetry conditions, it is sufficient to approximate only one hemisphere, resulting in formulations with 21 integration points. The corresponding geometry for which the microplanes are situated as tangential planes to the vertices and the edges of a regular icosahedron is depicted in Fig. 14.

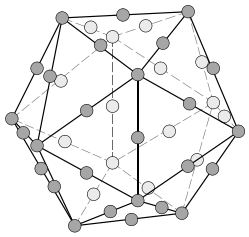

Fig. 14. Numerical integration with $n_{mp} = 21$ integration points per hemisphere.

References

Asaro, R.J., 1983. Crystal plasticity. J. Appl. Mech. 50, 921–934.

Batdorf, S.B., Budiansky, B., 1949. A mathematical theory of plasticity based on the concept of slip. Tech. Note 1871, National Advisory Committee for Aeronautics (NACA), Washington, DC.

Bažant, Z.P., Gambarova, P.G., 1984. Crack shear in concrete: crack band microplane model. J. Struct. Engng. ASCE 110, 2015–2036.

Bažant, Z.P., Oh, B.H., 1985. Microplane model for progressive fracture of concrete and rock. J. Engng. Mech. 111, 559–582.

Bažant, Z.P., Oh, B.H., 1986. Efficient numerical integration on the surface of a sphere. ZAMM 66 (1), 37–49.

Bažant, Z.P., Planas, J., 1998. Fracture and size effect in concrete and other quasibrittle materials. CRC Press, Boca Raton.

Bažant, Z.P., Prat, P., 1988. Microplane model for brittle plastic material: Part I – Theory, Part II – Verification. J. Engng. Mech. 114, 1672–1702.

Carol, I., Bažant, Z.P., 1997. Damage and plasticity in microplane theory. Int. J. Solids Struct. 34, 3807–3835.

Carol, I., Bažant, Z.P., Prat, P., 1991. Geometric damage tensor based on microplane model. J. Engng. Mech. 117, 2429–2448.

Carol, I., Jirásek, M., Bažant, Z.P., 2000a. A thermodynamically consistent approach to microplane theory. Part I: Free energy and consistent microplane stresses. Int. J. Solids Struct. 38(17)2921–2931.

Carol, I., Prat, P., Bažant, Z.P., 1992. New explicit microplane model for concrete: theoretical aspects and numerical implementation. Int. J. Solids Struct 29, 1173–1191.

Carol, I., Rizzi, E., Willam, K.J., 2000b. On the formulation of anisotropic elastic degradation. I: theory based on a pseudo-logarithmic damage tensor rate, and II: generalized pseudo-Rankine model for tensile damage. Int. J. Solids Struct., in press.

Lemaitre, J., 1992. A Course on Damage Mechanics. Springer, Berlin.

Lemaitre, J., Chaboche, J.L., 1985. Mechanique des Materiaux Solides. Dunod, Paris.

Lubarda, V., Krajcinovic, D., 1993. Damage tensors and the crack density distribution. Int. J. Solids Struct. 30, 2859–2877.

Ožbolt, J., Bažant, Z.P., 1992. Microplane model for cyclic triaxial behavior concrete. J. Engng. Mech. 118, 1365–1386.

Simo, J.C., Ju, J.W., 1987. Strain- and stress based continuum damage models: Part I – Formulation, Part II – Computational aspects. Int. J. Solids Struct. 23, 821–869.

Stroud, A.H., 1971. Approximate calculation of multiple integrals. Prentice Hall, Englewood Cliffs, NJ.

Taylor, G.I., 1938. Plastic strain in metals. J. Inst. Metals 62, 307–324.